

A density functional theory study for the Diels–Alder reaction between *N*-acyl-1-aza-1,3-butadienes and vinylamines. Lewis acid catalyst and solvent effects

Luis Ramón Domingo*

Departamento de Química Orgánica, Instituto de Ciencia Molecular, Universidad de Valencia, Dr Moliner 50, Burjassot, 46100 Valencia, Spain

Received 5 December 2001; revised 1 March 2002; accepted 18 March 2002

Abstract—The molecular mechanism for the Diels–Alder reaction of *N*-acyl-1-aza-1,3-butadiene with dimethylvinylamine has been studied using density functional theory methods. This cycloaddition is the nucleophilic attack of the vinylamine to the conjugate position of the unsaturated acyl imine with concomitant ring-closure. The presence of a Lewis acid catalyst coordinated to the acyl oxygen atom decreases markedly the activation energy associated to the nucleophilic attack. This results from an increasing of the electrophilicity of the 1-aza-1,3-butadiene that shift the mechanism from a highly asynchronous concerted process to a polar stepwise one. © 2002 Elsevier Science Ltd. All rights reserved.

1. Introduction

The Diels–Alder reaction of 1-aza-1,3-butadienes (1ABD) is a valuable methodology for synthesis of nitrogen heterocycles^{1–3} bearing endocyclic enamine moieties that are key intermediates in the preparation of complicated heterocycles⁴ and natural products.⁵ The Diels–Alder participation of simple 1ABD is rarely observed in normal [4+2] cycloaddition reactions; however, this problem can be circumvented by introducing either electron-withdrawing or electron-donating substituents onto the nitrogen atom. Fowler^{4,5} and Boger^{6,7} have shown that the inclusion of a strong electron-withdrawing acyl *o* sulfonyl group onto the nitrogen atom favor considerably the inverse-electron-demand Diels–Alder (IEDDA) reactivity of the desired azabutadienes. Boruah et al.⁸ have described recently the IEDDA reaction of the *N*-acyl-4-chloro-1-aza-butadiene **1** with a series of vinylamines **2** to give the derivatives **4**. This sequential reaction is initialized by a [4+2] cycloaddition between **1** and **2** to give the intermediate **3**, which affords in the reaction conditions the final derivative **4** (Scheme 1).⁸ In addition, this reaction is manifestly catalyzed with the presence of TiCl₄ or BF₃·OEt₂ Lewis acids (LA).

The hetero-Diels–Alder reactions have been comparatively less studied from a theoretical point of view than the Diels–Alder ones. Several theoretical works devoted to the study of the aza-Diels–Alder (ADA) reaction using azabutadiene

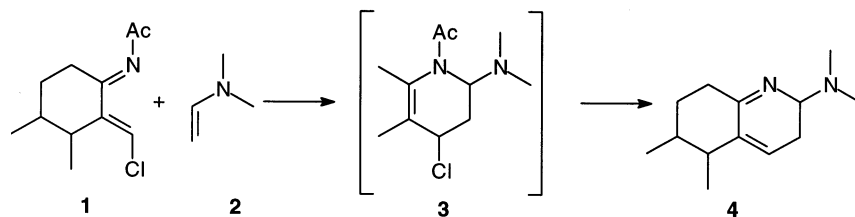
systems: 1-azabutadienes,^{6,9–12} 2-azabutadienes,^{10,13–17} 1,2-diazabutadienes,^{18,19} and 2,3-diazabutadienes²⁰ have been reported in literature.

The ADA reaction of (*E*)-1-aza-1,3-butadiene with ethylene has been widely studied. Riche and co-workers⁹ studied this reaction at the RHF/STO-3G and RHF/3-21G computational levels, finding transition structures (TS) corresponding to a concerted process where the C–C distance, 2.158 Å, is slightly shorter than the N–C one, 2.103 Å (3-21G results). A similar bond-formation was found for Bachrach et al.¹⁰ at the MP2/6-31G* level. The activation energy for the (*E*)-isomer was found 3.6 kcal/mol less energetic than for the (*Z*)-one.¹⁰ Lee et al.¹¹ have studied recently several ADA reactions finding similar results for the (*E*)-1-aza-1,3-butadiene and ethylene cycloaddition reaction. The C–C and N–C distances at the TS using the B3LYP/6-31G* computational level are 2.163 and 2.196 Å, respectively. These distances point out to a concerted process where the C–C bond-formation is slightly more advanced than the C–N one. These authors suggest that a terminal nitrogen atom in the diene lower the LUMO level sufficiently to make the reaction an inverse-electron-demanding one. This cycloaddition presents a large barrier; 21.8 and 26.3 kcal/mol for the (*E*)- and (*Z*)-1-aza-1,3-butadiene, respectively.

Tietze and co-workers¹² have studied the concerted and stepwise mechanisms for the ADA reaction of (*E*)-1-aza-1,3-butadiene with ethylene at the UHF/6-31G* level. These calculations show that the stepwise mechanism with a large diradicaloid character is favored over the concerted

Keywords: aza-Diels–Alder reactions; Lewis acid catalysts; solvent effects; molecular mechanism; density functional theory calculations.

* Fax: +34-96-398-3152; e-mail: domingo@utopia.uv.es



Scheme 1.

one. While the C–C and N–C distances at the concerted TS are 2.082 and 2.139 Å (RHF/6-31G* results), respectively, at the TS corresponding to the stepwise attack of ethylene to 1ABD are 2.023 and 3.580 Å (UHF/6-31G* results).

The IEDDA reaction of (*E*)-*N*-sulfonyl-1-aza-1,3-butadiene with electron-rich vinyl ethers has been studied by Boger and co-workers⁶ both experimentally and theoretically using the frontier molecular orbital (FMO) model. These cycloadditions cleanly provide one Diels–Alder cycloadduct, and the reaction proved to proceed predominantly if not exclusively ($\geq 95\%$) through an *endo* transition state. An AM1 FMO analysis for these 1ABDs and methyl vinyl ether clearly support the observation of expected *ortho* regio- and *endo*-stereoselectivity for these cycloadditions. Thus, the magnitude of the LUMO_{diene} C4 coefficient proved largest of the diene termini supporting the *ortho* regioselectivity experimentally observed.⁶

Recently, we have studied the ADA reaction of two iminium cations with cyclopentadiene, Cp,^{21,22} within of our research program devoted to the study of cycloaddition reactions which can take place along polar processes instead of pericyclic ones.^{23–28} These studies point out that these formally [4+2] cycloadditions are the nucleophilic attack of Cp to the strong electrophilic iminium cations with concomitant ring-closure.²¹ The ionic character showed by the large

charge transfer at the TSs accounts for the lowering of the activation energy for these formally [4+2] cycloadditions.

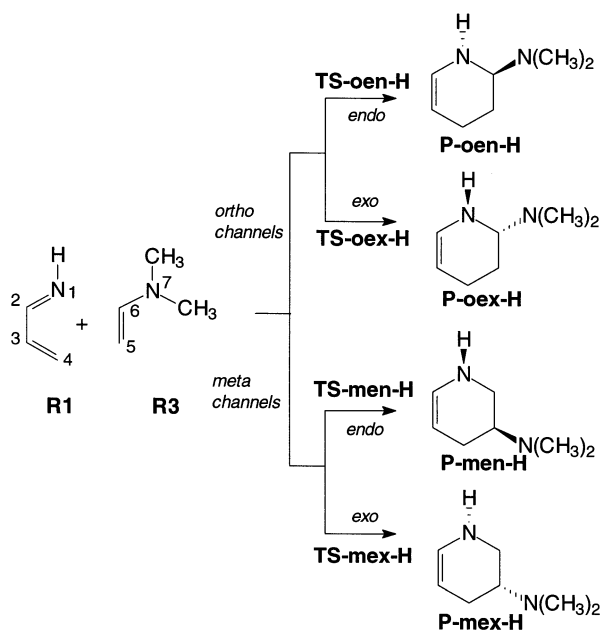
In this paper we present herein the results of a density functional theory^{29–31} (DFT) study on the IEDDA reaction between (*E*)-1-aza-1,3-butadiene, **R1**, and (*E*)-*N*-acyl-1-aza-1,3-butadiene, **R2**, with dimethylvinylamine, **R3**, in order to explaining the effect of the acyl substitution on these ADA reactions (see Schemes 2 and 3). The reaction of the BH₃ coordinated (*E*)-*N*-acyl-1-aza-1,3-butadiene, **R2-B**, with **R3** has been also studied to understanding the role of the Lewis acid catalysts in these ADA reactions (see Scheme 4). Our purpose is to contribute to a better understanding of the mechanistic features of these cycloaddition processes, especially by location and characterization of all stationary points involved at the reaction. Finally, a density function theory analysis at these reactions has been also carried out in order to explain both reactivity and regioselectivity.

2. Global and local properties

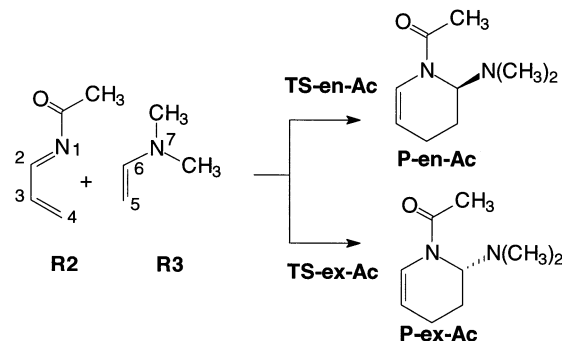
Global electronic indexes, as defined within the DFT of Parr, Pearson and Yang^{29,30} are useful tools to understand the reactivity of molecules in their ground states. For instance, the electronic chemical potential μ describing the changes in electronic energy with respect to the number of electrons is usually associated with the charge transfer ability of the system in its ground state geometry. It has been given a very simple operational formula in terms of the one-electron energies of the FMO HOMO and LUMO, ε_H and ε_L , as:

$$\mu \approx \frac{\varepsilon_H + \varepsilon_L}{2} \quad (1)$$

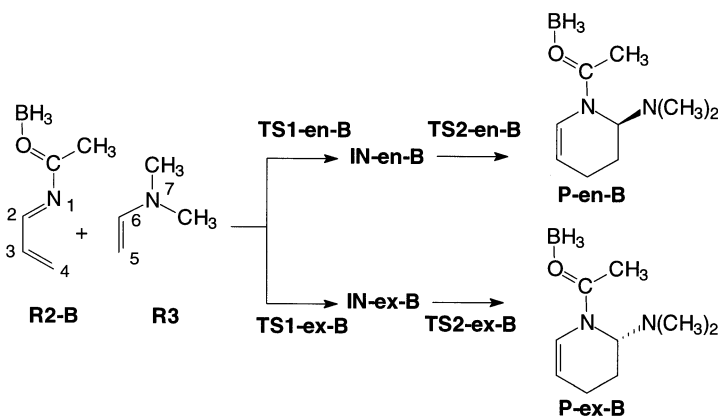
Besides this index, it is also possible to give a quantitative representation to the chemical hardness concept introduced



Scheme 2.



Scheme 3.



Scheme 4.

by Pearson,³² which may be represented as:³⁰

$$\eta \approx \varepsilon_L - \varepsilon_H \quad (2)$$

Recently, Parr et al.³³ have introduced a new and useful definition of global electrophilicity, which measures the stabilization in energy when the system acquires an additional electronic charge ΔN from the environment. The electrophilicity power has been given by the following simple expression:³³

$$\omega = \frac{\mu^2}{2\eta} \quad (3)$$

in terms of the electronic chemical potential μ and the chemical hardness η , defined in Eqs. (1) and (2).

Recent studies for the electrophilicity of common diene/dienophile pair in Diels–Alder reactions have shown that the classification of these reagents in an unique scale of electrophilicity, ω , is a powerful tool to predict the ionicity of the cycloaddition process, and in consequence, its feasibility.^{34–36} Thus, the difference of electrophilicity, $\Delta\omega$, for a diene/dienophile pair located at the extremes of the electrophilicity scale agrees with a process with a large ionic character. Moreover, evaluation of the local electrophilic and nucleophilic Fukui functions³⁷ at the reagents allows explaining the regioselectivity observed for a polar process.³⁵

3. Computational methods

DFT calculations have been carried out using the B3LYP^{38,39} exchange–correlation functionals, together with the standard 6-31G* basis set.⁴⁰ The optimizations were carried out using the Bery analytical gradient optimization method.^{41,42} The stationary points were characterized by frequency calculations in order to verify that the TS have one and only one imaginary frequency. The intrinsic reaction coordinate (IRC)⁴³ path was traced in order to check the energy profiles connecting each transition structure to the two associated minima of the proposed mechanism by using the second order González–Schlegel integration method.^{44,45} The electronic structures of stationary points were analyzed by the natural bond orbital (NBO) method.^{46,47} All calculations were carried out with the

Gaussian 98 suite of programs.⁴⁸ Optimized geometries of all structures are available from the author.

The solvent effects have been considered optimizing the B3LYP/6-31G* gas phase stationary points using a relatively simple self-consistent reaction field (SCRF) method^{49,50} based on the polarizable continuum model (PCM) of the Tomasi's group.^{51–53} The solvent used in the experimental work is dichloromethane. Therefore, we have used the dielectric constant at 298.0 K, $\varepsilon=8.93$.

Electrophilic and nucleophilic Fukui functions³⁷ condensed to atoms have been evaluated from single point calculations performed at the ground state of molecules at the same level of theory, using a method described elsewhere.^{54,55} This method evaluates Fukui functions using the coefficients of the FMOs involved in the reaction and the overlap matrix. The global electrophilicity power was evaluated using Eq. (3) with the electronic chemical potential and chemical hardness given by Eqs. (1) and (2).

4. Results and discussions

In the first part energetic aspects, geometrical parameters of TSs and their electronic structure in terms of bond orders and natural charges for the cycloaddition reaction of 1-aza-1,3-butadiene and its corresponding acyl derivative with dimethylvinylamine will be analyzed (Sections 4.1 and 4.2). In the second part the role of the BH₃ LA catalyst will be rationalized (Section 4.3). In the third part, the solvent effects on these cycloadditions will be discussed (Section 4.4). Finally, a DFT analysis for both reactivity and regioselectivity will be performed (Section 4.5).

4.1. Study of the cycloaddition reaction between (E)-1-aza-1,3-butadiene **R1** and dimethylvinylamine **R3**

The cycloaddition reaction between (E)-1-aza-1,3-butadiene **R1** and the vinylamine **R3** can take place along four reactive channels corresponding to the *endo* and *exo* approach modes of the amine nitrogen atom of **R3** relative to the 1ABD system of **R1** in two regioisomeric possibilities, *ortho* (head-to-head) and *meta* (head-to-tail) pathways (see Scheme 2). The stereoisomeric channels along the *ortho* pathways correspond to the N1–C6 and

Table 1. Total energies (au, for **R3** –212.562345 au) and relative energies (kcal/mol, in parentheses, relative to *s-trans* **R1**+**R3**, *s-trans* **R2**+**R3**, and *s-trans* **R2-B**+**R3**) for the stationary points corresponding to the cycloaddition reaction of 1-aza-1,3-butadiene, **R1**, *N*-acyl-1-aza-1,3-butadiene, **R2**, and BH₃ coordinated *N*-acyl-1-aza-1,3-butadiene, **R2-B**, with dimethylvinylamine, **R3**

<i>s-trans</i> R1	–172.034903	<i>s-trans</i> R2	–324.689836	<i>s-trans</i> R2-B	–351.334628
<i>s-cis</i> R1	–172.030408 (2.8)	<i>s-cis</i> R2	–324.685799 (2.5)	<i>s-cis</i> R2-B	–351.330676 (2.5)
TS-oen-H	–384.565197 (20.1)	TS-en-Ac	–537.235854 (10.2)	TS1-en-B	–563.893674 (2.1)
TS-oex-H	–384.566241 (19.5)	TS-ex-Ac	–537.231027 (13.3)	TS1-ex-B	–563.888929 (5.0)
TS-men-H	–384.546757 (31.7)	P-en-Ac	–537.300757 (–30.5)	IN-en-B	–563.916784 (–12.4)
TS-mex-H	–384.546717 (31.7)			IN-ex-B	–563.911145 (–8.9)
P-oen-H	–384.645028 (–30.0)			TS2-en-B	–563.916498 (–12.3)
P-men-H	–384.636166 (–24.4)			TS2-ex-B	–563.910616 (–8.6)
				P-en-B	–563.943130 (–29.0)

C4–C5 forming bond processes, whereas the *meta* pathways correspond to the N1–C5 and C4–C6 ones.

Analysis of the results renders that the cycloaddition between **R1** and **R3** takes place along a highly asynchronous concerted mechanism. Thus, four TSs, **TS-oen-H**, **TS-oex-H**, **TS-men-H** and **TS-mex-H**, and four cycloadducts, **P-oen-H**, **P-oex-H**, **P-men-H** and **P-mex-H**, corresponding to the *endo* and *exo* channels, name as *en* and *ex*, along the *ortho* and *meta* pathways, name as *o* and *m*, respectively, have been found and characterized. The stationary points corresponding to the cycloaddition reaction between **R1** and **R3** have been presented in Scheme 2 together with the atom numbering, while the total and relative energies are summarized in Table 1. The geometries of the TSs are presented in Fig. 1.

For the 1ABD derivatives there is two configurational isomers corresponding to the (*E*) and (*Z*) arrangements of the imine framework. Although for a small hydrogen atom both isomers present similar energies, the presence of a bulky acyl substituent on the N1 nitrogen atom on **R2** and **R2-B** prevents the (*Z*) arrangement. In addition, for these acyclic 1ABD derivatives two conformations are possible corresponding to the *s-cis* and *s-trans* arrangement of the 1ABD system around the C2–C3 single bond. The *s-trans*

conformations are between 2.5 and 2.8 less energetic than the *s-cis* ones. However, the low rotational barrier around the C2–C3 single bond allows at the experimental conditions the easy equilibrium between both conformers. In consequence, the *s-cis* arrangement for the (*E*)-1-aza-1,3-butadiene derivatives have been chosen along the present study.

The values of the relative energies for **TS-oen-H**, **TS-oex-H**, **TS-men-H** and **TS-mex-H**, with respect to separate reactants, the *s-trans* conformation of **R1** and **R3**, are 20.1, 19.5, 31.7 and 31.7 kcal/mol, respectively. These barriers reveal that the *ortho* approaches are favored over the *meta* ones; the **TS-oen-H**, and **TS-oex-H** are ca. 12 kcal/mol less energetic than **TS-men-H** and **TS-mex-H**. Therefore, there is a pronounced *ortho* regioselectivity for this ADA reaction. The stereoselectivity measured as the difference of barriers between the *endo* and *exo* TSs for the more favorable *ortho* attack mode indicates that in gas phase this reaction presents a slightly *exo* selectivity; **TS-oen-H** is 0.6 kcal/mol more energetic than **TS-oex-H**. This cycloaddition presents a lower barrier than that for the cycloaddition between 1,3-butadiene and the vinylamine **R3**, 27.1 kcal/mol, and for the cycloaddition between **R1** and ethylene,¹¹ 21.8 kcal/mol. Thus, the presence of the electro-negative N1 nitrogen atom on the 1,3-butadiene system that

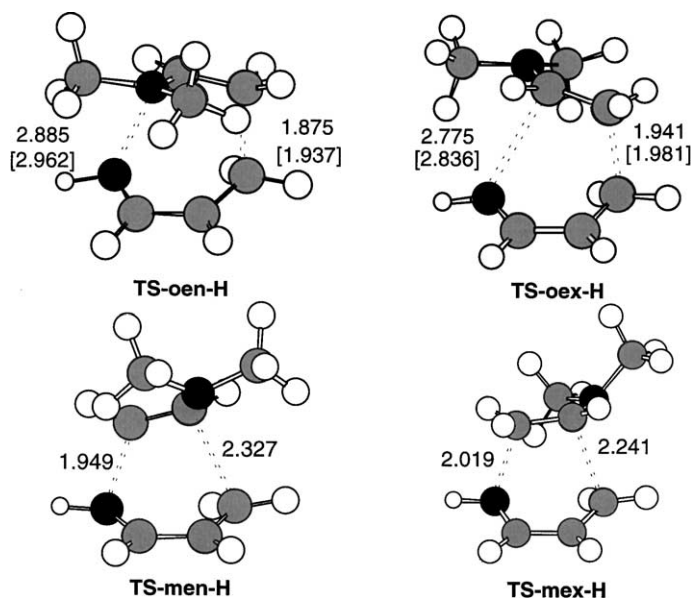


Figure 1. TS corresponding to the cycloaddition reaction between 1-aza-butadiene, **R1**, and dimethylvinylamine, **R3**. The values of the lengths of the bonds directly involved in the reaction obtained at the B3LYP/6-31G*, and B3LYP/6-31G* in dichlorometane [] are given in angstroms.

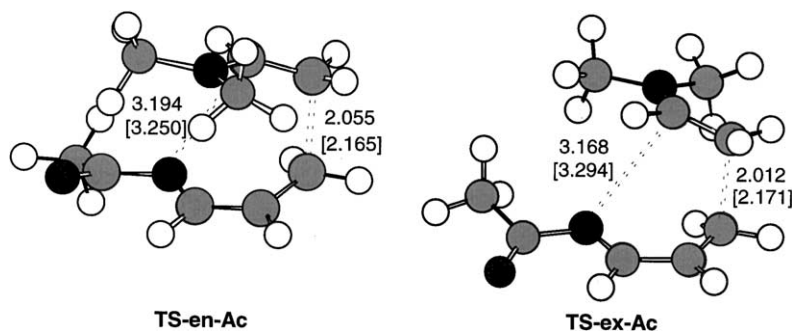


Figure 2. TS corresponding to the cycloaddition reaction between *N*-acyl-1-aza-butadiene, **R2**, and dimethylvinylamine, **R3**. The values of the lengths of the bonds directly involved in the reaction obtained at the B3LYP/6-31G*, and B3LYP/6-31G* in dichlorometane [] are given in angstroms.

constitutes an α,β -unsaturated imine increases the electrophilicity of the 1ABD system favoring the reaction with the electron-rich vinylamine along the *ortho* reactive channel.

From these TSs the related minima associated with the final cycloadducts can be obtained. The *ortho* cycloadducts, **P-oen-H** and **P-oex-H**, and *meta* ones, **P-men-H** and **P-oex-H**, are two pair of enantiomers with identical energy due to the easy inversion on the N1 nitrogen atom belonging to the vinylamine system present on the cycloadducts. All cycloaddition pathways are very exothermic processes, between -30 and -24 kcal/mol, respectively, the *ortho* cycloadducts are ca. 6 kcal/mol more stable than the *meta* ones.

For the more favorable *ortho* TSs, the lengths of the C4–C5 forming bonds, 1.875 Å at **TS-oen-H** and 1.941 Å at **TS-oex-H**, are shorter than the lengths of the N1–C6 ones, 2.885 Å at **TS-oen-H** and 2.775 Å at **TS-oex-H**. These bond lengths indicate that the *ortho* TSs correspond with concerted but highly asynchronous bond-formation processes where the C4–C5 forming bond is being formed in a larger extension than the N1–C6 one. This behavior is a consequence of the large polarization of C3–C4 double bond belonging to the 1ABD that makes the C4 atom the more electrophilic center, and the large polarization of the C5–C6 double bond of **R3** because of the presence of the electron-donating amine group that makes the C5 carbon atom the more nucleophilic one (see Section 4.5). Different results are obtained for the *meta* TSs where the lengths of the N1–C5 and C4–C6 forming bond are ca. 2.0 and 2.3 Å, respectively. These TSs correspond with asynchronous concerted bond-formation where the bond at the β -position of the vinylamine is formed in a large extension. Thus, the more favorable interaction between the C4 atom, the more electrophilic center of **R1**, and the C5 atom, the more nucleophilic one of **R3**, along the *ortho* channels allows explaining the large regioselectivity found at this cycloaddition (see Section 4.5).

The extent of bond-formation along a reaction pathway is provided by the concept of bond order (BO).⁵⁶ The BO values of the N1–C6 and C4–C5 forming bonds along the *ortho* reactive channels are 0.12 and 0.61 at **TS-oen-H** and 0.14 and 0.55 at **TS-oex-H**, respectively, while the BO values of the N1–C5 and C4–C6 forming bonds along the *meta* ones are 0.50 and 0.34 at **TS-men-H** and 0.56 and 0.37 at **TS-mex-H**, respectively. These BOs show a larger

asynchronicity on the bond-formation process at the more favorable *ortho* TSs as a consequence of the large interaction between the more electrophilic C4 and nucleophilic C5 centers of **R1** and **R3**, respectively, along the C4–C5 bond-formation.

Since this cycloaddition presents asynchronous TSs diradical structures could in principle be involved.¹² This has been ruled out by obtaining the wave functions of the TSs with unrestricted DFT theory. UB3LYP/6-31G* calculations, using the keyword STABLE in Gaussian 98, predict the same structures as the ones obtained from the restricted B3LYP/6-31G*, indicating that the restricted DFT solutions are stable, allowing to rule out the presence of diradical species.^{27,57–59}

Finally, the natural population analysis⁴⁶ (NPA) allows us to evaluate the charge transferred along the cycloaddition process. The B3LYP/6-31G* atomic charges at the TSs have been shared between the donor vinylamine **R3** and the acceptor 1ABD **R1**. The values of the charge transferred from **R3** to **R1** are 0.37e and 0.39e at the *endo* and *exo ortho* TSs, respectively, while these for the *endo* and *exo meta* TSs are 0.17e and 0.14e, respectively. These data indicate a larger charge transfer along the more favorable *ortho* TSs that fluxes from the electron-rich vinylamine to the electron-poor 1ABD.

4.2. Study of the cycloaddition reaction between (*E*)-*N*-acyl-1-aza-1,3-butadiene **R2** and dimethylvinylamine **R3**

The cycloaddition reaction between (*E*)-*N*-acyl-1-aza-1,3-butadiene **R2** and the vinylamine **R3** can take place also along four reaction pathways corresponding to the *endo* and *exo* approach modes of the amine nitrogen atom of **R3** to the 1ABD system of **R1** along the *ortho* and *meta* regioisomeric pathways. However, the large *ortho* regioselectivity that present these cycloadditions allows us to discard the study of the *meta* reactive channels (see Section 4.1). Analysis of the results renders that this cycloaddition takes place along a concerted but highly asynchronous mechanism. Thus, two TSs, **TS-en-Ac** and **TS-ex-Ac**, and two cycloadducts, **P-en-Ac** and **P-ex-Ac**, corresponding to the *endo* and *exo ortho* reactive channels, respectively, have been found and characterized. The stationary points corresponding to the cycloaddition reaction between **R2** and **R3** have been presented in Scheme 3 together with the atom numbering, while the total and relative energies are

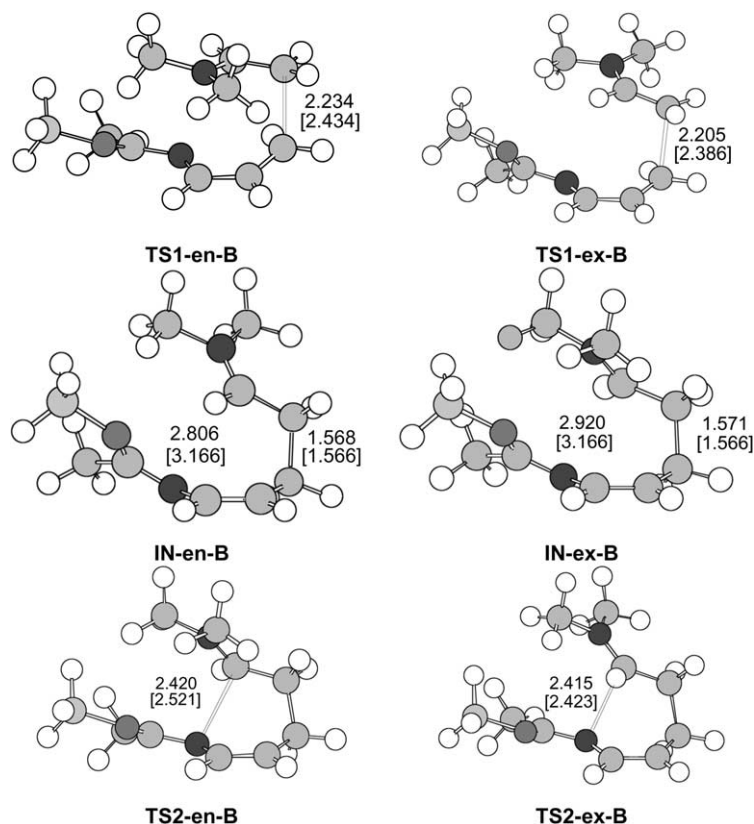


Figure 3. TS and intermediates corresponding to the LA catalyzed cycloaddition reaction between BH_3 coordinated *N*-acyl-1-aza-butadiene, **R2-B**, and dimethylvinylamine, **R3**. The values of the lengths of the bonds directly involved in the reaction obtained at the B3LYP/6-31G*, and B3LYP/6-31G* in dichlorometane [] are given in angstroms.

summarized in Table 1. The geometries of these TSs are presented in Fig. 2.

The values of the relative energies for **TS-en-Ac** and **TS-ex-Ac**, with respect to separate reactants, *s-trans* conformation for **R2** and **R3**, are 10.2 and 13.3 kcal/mol, respectively. A comparison of the barriers for the cycloadditions of **R1** and **R2** with **R3** shows that the acylation of the nitrogen atom decreases markedly the barrier for the cycloaddition, as well changes the stereoselectivity. Thus the barrier for **TS-en-Ac** is 9.3 kcal/mol less energetic than that for **TS-oex-H**. In addition, the *endo* **TS-en-Ac** is 3.1 kcal/mol less energetic than the *exo* **TS-ex-Ac**; therefore, in gas phase this cycloaddition presents a large *endo* stereoselectivity.

The lengths of the N1–C6 and C4–C5 forming bonds at the *endo* **TS-en-Ac** are 3.194 and 2.055 Å, respectively, while at the *exo* **TS-ex-Ac** the corresponding values are 3.168 and 2.012 Å, respectively. These bond lengths indicate that both TSs correspond with highly asynchronous bond-formation processes where only the C4–C5 bond is being formed; a distance of 3.2 Å precludes any covalent interaction. The BO values of the N1–C6 and C4–C5 forming bonds are 0.04 and 0.46 at **TS-en-Ac** and 0.05 and 0.49 at **TS-ex-Ac**, respectively. These BOs show that only the C4–C5 bond is being formed at these TSs. Finally, the values of the charge transferred from **R3** to **R2** are 0.39e and 0.38e at the *endo* and *exo* TSs, respectively. These results indicate also a large charge transfer along the cycloaddition that fluxes from the electron-rich vinylamine to the electron-

poor activated *N*-acyl-1-azabutadiene. The NPA shows a similar charge transfer than that for the reaction between **R1** and **R3**. However, the presence of the acyl group on **R3** allows a favorable delocalization of the charge transferred at the TSs increasing the electrophilicity of **R2** relative to **R1**, and decreasing the barrier heights (see Section 4.5).

4.3. Study of the BH_3 catalyzed reaction between **R2-B** and **R3**

As it was stated in Section 1, these ADA reactions are catalyzed by the presence of a Lewis acid. Our next step was the study of the role of the LA on the mechanism of the reaction. The effect of the LA catalysts on these ADA reactions has been considered studying the cycloaddition between the BH_3 coordinated *N*-acyl-1-aza-1,3-butadiene **R2-B** and the vinylamine **R3**. In this reaction model the boron atom has been coordinated to the acyl oxygen atom. Analysis of the results indicates that the presence of the LA changes manifestly the mechanism. The LA catalyzed cycloaddition takes place along a stepwise process. The first step corresponds with the nucleophilic attack of the C5 carbon atom of the vinylamine **R3** to the C4 carbon atom of the BH_3 coordinated *N*-acyl-1-azabutadiene **R2-B** to give an acyclic zwitterionic intermediate. The second step corresponds with the ring-closure process at this intermediate to give the final formally [4+2] cycloadduct. In addition, for the nucleophile attack two reactive channels, the *endo* and *exo*, are feasible along the *ortho* pathways.

Table 2. Total energies (au, for **R3-S** –212.563970 au) and relative energies (kcal/mol, in parentheses, relative to *s-trans* **R1-S**+**R3-S**, *s-trans* **R2-S**+**R3-S**, and *s-trans* **R2-B-S**+**R3-S**) for the stationary points corresponding to the cycloaddition reaction of 1-aza-1,3-butadiene, **R1-S**, *N*-acyl-1-aza-1,3-butadiene, **R2-S**, and BH₃ coordinated *N*-acyl-1-aza-1,3-butadiene, **R2-B-S**, with dimethylvinylamine, **R3-S**, in dichloromethane

<i>s-trans</i> R1-S	–172.038944	<i>s-trans</i> R2-S	–324.693959	<i>s-trans</i> R2-B-S	–351.343154
TS-oen-H-S	–384.571797 (19.5)	TS-en-Ac-S	–537.243746 (8.9)	TS1-en-B-S	–563.904814 (1.4)
TS-oex-H-S	–384.571442 (19.7)	TS-ex-Ac-S	–537.241575 (10.3)	TS1-ex-B-S	–563.902239 (3.1)
P-oen-H-S	–384.648135 (–28.4)	P-en-Ac-S	–537.306711 (–30.6)	IN-en-B-S	–563.935622 (–17.9)
				IN-ex-B-S	–563.934104 (–16.9)
				TS2-en-B-S	–563.935571 (–17.9)
				TS2-ex-B-S	–563.934143 (–17.0)
				P-en-B-S	–563.955479 (–30.3)

Thus, two TSs for the nucleophilic attack associated with the C4–C5 bond formation, **TS1-en-B** and **TS1-ex-B**, two acyclic zwitterionic intermediates, **IN-en-B** and **IN-ex-B**, two TSs for the ring-closure process associated with the N1–C6 bond-formation, **TS2-en-B** and **TS2-ex-B**, and two cycloadducts, **P-en-B** and **P-ex-B**, associated to the *endo* and *exo* channels, respectively, are been located and characterized. The stationary points corresponding to the BH₃ catalyzed cycloaddition reaction between **R2-B** and **R3** have been presented in Scheme 4 together with the atom numbering, while the total and relative energies are summarized in Table 1. The geometries of the TSs and intermediates are presented in Fig. 3.

The barriers associated to the nucleophilic attack of the vinylamine **R3** to the BH₃ coordinated *N*-acyl-1-azabutadiene **R2-B** along the *endo* and *exo* reactive channels are 2.1 and 5.1 kcal/mol, respectively. Therefore, there is a strong decreasing of the activation energy for the LA catalyzed reaction relative to the uncatalyzed one; **TS1-en-B** is 8.1 kcal/mol less energetic than **TS-en-Ac**. These results indicate that these cycloadditions are clearly catalyzed by the presence of Lewis acids in agreement with the experimental results.⁸ In addition, **TS1-en-B** is 2.9 kcal/mol less energetic than **TS1-ex-B**. In consequence, the LA catalyzed cycloaddition presents also large *endo* selectivity. This finding that is also observed in other polar stepwise cycloadditions^{22,35} allows us to rule out the widespread opinion that a large *endo* selectivity for the Diels–Alder reactions indicates a pericyclic concerted bond-formation process.

For the TSs corresponding to the nucleophilic attack of **R3** to **R2-B** the lengths of the C4–C5 forming bond are 2.234 Å for **TS1-en-B** and 2.205 Å for **TS1-ex-B**, while the distance between the N1 nitrogen and C6 carbon atoms become 3.339 Å for **TS1-en-B** and 3.367 Å for **TS1-ex-B**. These distances are slightly larger than those found at the highly asynchronous **TS-en-Ac** and **TS-ex-Ac**. The C4–C5 bond lengths at the corresponding intermediates are 1.568 and 1.571 Å, respectively, while the N1–C6 distances are 2.806 and 2.920 Å. Finally, at the TSs corresponding to the ring-closure process the lengths of the N1–C6 forming bonds are 2.420 Å for **TS2-en-B**, and 2.415 Å for **TS2-ex-B**.

The C4–C5 BO values at **TS1-en-B** and **TS1-ex-B** are 0.34 and 0.36, respectively, while the N1–C6 BO values are 0.02 and 0.03, respectively. At the intermediates **IN-en-B** and **IN-ex-B** the C4–C5 BO values, 0.95 and 0.96, respectively, indicate that these C–C single bonds are already formed,

while the N1–C6 BOs remain to 0.07 and 0.06, respectively. The C6–N7 BO values at these intermediates, 1.58 and 1.57, respectively, point out a large π character for the C6–N7 bond as a consequence of the large delocalization of the N7 lone pair on the C6 carbon atom belonging to the ethylene framework. This allows a large stabilization of the positive charge that has been developed at the C6 carbon atom at these zwitterionic intermediates. This behavior allows explaining the large nucleophilic character of the vinylamine **R3** that acts as a strong nucleophile. Finally, at **TS2-en-B** and **TS2-ex-B** the N1–C6 BO values are 0.18 and 0.19, respectively.

The values of the charge transferred from **R3** to **R2-B** along the *endo* and *exo* stepwise pathways are 0.37e (**TS1-en-B**), 0.36e (**TS1-ex-B**), 0.77e (**IN-en-B**), 0.78e (**IN-ex-B**), 0.70e (**TS2-en-B**) and 0.69e (**TS2-ex-B**). These values show an increase of the charge transferred along the nucleophilic attack of the vinylamine **R3** to the BH₃ coordinated *N*-acyl-1-azabutadiene **R2-B** up to formation of the zwitterionic intermediates **IN-en** and **IN-ex**. In addition, the charge transfer along the more favorable *endo* TSs are slightly larger than that for *exo* one.²⁷ Thus, the favorable coulombic interactions that appear at the *endo* zwitterionic **TS1-en-B** favor the charge transfer, decreasing the activation energy relative the *exo* one.

Finally, a comparative analysis of the electronic structures based in BOs and charge transfers for the TSs corresponding to the concerted reaction between **R2** and **R3**, **TS-en-Ac** and **TS-ex-Ac**, with those associated to the nucleophilic attack of **R3** to **R2-B**, **TS1-en-B** and **TS1-ex-B**, shows similar bond-formation processes. In consequence, the concerted TSs must be associated to a polar process characterized by the nucleophilic attack of **R3** to the conjugate position of the unsaturated *N*-acyl-imine **R2** without the participation of any zwitterionic intermediate because of the non-existence of an appreciable barrier for the cyclization process.²¹ Note that the stepwise cycloaddition has a negligible barrier for the ring-closure step. However, the presence of the intermediates along the reaction paths allow us to classify **TS1-en-B** and **TS1-ex-B** as TSs associated to one-center additions instead of [4+2] processes.⁵⁹

4.4. Solvent effects

Solvent effects on cycloaddition reactions are well known and have received considerable attention, especially in the last few years. As solvent can modify both activation energy and *endo/exo* selectivity, its effect on the reaction can give an useful information about the mechanism. In

Table 3. Global properties (electronic chemical potential, μ , and chemical hardness, η , values are in au; electrophilicity power values, ω , are in eV) of same dienes and dienophiles involved on inverse-electron-demand Diels–Alder reactions of 1-azabutadiene derivatives

Molecule	μ	η	ω
1-Acyl-1-aza-1,3-butadiene-BH ₃ R2-B	-0.1855	0.1446	3.24
1-Sulfonyl-1-aza-1,3-butadiene	-0.1825	0.1946	2.33
1-Acyl-1-aza-1,3-butadiene R2	-0.1625	0.1680	2.14
1-Aza-1,3-butadiene R1	-0.1505	0.2100	1.47
1,3-Butadiene	-0.1270	0.2083	1.05
Ethylene	-0.1239	0.2855	0.73
Methyl vinyl ether	-0.0894	0.2564	0.42
Dimethylvinylamine R3	-0.0680	0.2390	0.27

consequence, the solvent effects at the relative energies have been evaluated by geometrical optimization on the gas phase B3LYP/6-31G* geometries using a relatively simple SCRF method^{49,50} based on the PCM method of Tomasi's group,^{51–53} together with the dielectric constant of dichloromethane, $\epsilon=8.93$. Table 2 reports the total and relative energies of the optimized stationary points corresponding to the cycloaddition reaction of **R1**, **R2** and **R2-B** with **R3** obtained by the SCRF method.

With the inclusion of the solvent effects the TSs and intermediates are more stabilized relative to reactants due to the large charge transfer that is being developed along these cycloadditions. Thus, the solvent effects decrease the barriers in ca. 1–2 kcal/mol. Similar results are found for the three cycloadditions studied here in agreement with the similar charge transfer found at the TSs associated with the attack of **R3** to the 1ABD derivatives **R1**, **R2** and **R2-B**. In dichloromethane the cycloaddition between **R1** and **R3** is lightly *endo* selective as a consequence of the larger solvation of **TS-oen-H-S** than **TS-oex-H-S**. On the other hand, the inclusion of solvent effects decrease lightly the large *endo* selectivity found in gas phase for the LA catalyzed process; now **TS-en-B-S** is 1.7 kcal/mol less energetic than **TS-ex-B-S**.

A comparison of the geometrical parameters of the TSs given in Figs. 1–3 shows that the inclusion of solvent effects on the geometry optimization does not modify substantially the geometries obtained in gas phase.²¹ These results are a consequence of the high asynchronicity on the bond-formation found in gas phase that is not modify with the inclusion of solvent effects. The lengths of the forming bonds obtained in gas phase are between 0.05 and 0.20 Å shorter than those obtained with the SCRF method. Thus, the

Table 4. Fukui functions for nucleophilic (+) and electrophilic (–) attacks for the 1-azabutadienes **R1**, **R2**, and **R2-B**, and the vinylamine **R3**

Fukui functions for nucleophilic (+) attacks					
	N1	C2	C3	C4	(a)
R2-B	0.15	0.30	0.05	0.28	0.77
R2	0.18	0.28	0.08	0.30	0.84
R1	0.27	0.23	0.14	0.35	1.00
Fukui functions for electrophilic (–) attacks					
	C5	C6	N7		
R3	0.41	0.09	0.39		

(a) Fukui functions condensed on the azadiene system.

stabilization of the TSs by the inclusion of solvent effects leads to earlier TSs.

4.5. Global and local electrophilicity/nucleophilicity analysis

Finally, these cycloaddition reactions have been also analyzed using the global and local indexes defined in the context of the DFT.^{29–31} Recent studies carried out by us on cycloaddition reactions with a large polar character have shown that these indexes are powerful tools to study both reactivity and regioselectivity.^{34–36} In Table 3 the static global properties, electronic chemical potential μ , chemical hardness η , and global electrophilicity ω , defined in Eqs. (1)–(3), for the 1ABDs **R1**, **R2** and **R2-B** and the vinylamine **R3** are displayed.

The electronic chemical potential of 1-aza-1,3-butadiene **R1** ($\mu=-0.1505$ au) is less than the electronic chemical potential of dimethylvinylamine **R3** ($\mu=-0.0680$ au) thereby indicating that the net charge transfer will take place from **R3** towards **R1**, in agreement with the charge transfer analysis (see Section 4.1), and with an IEDDA reactivity. 1-Aza-1,3-butadiene, **R1**, has a larger electrophilicity power, $\omega=1.47$ eV, than 1,3-butadiene, $\omega=1.05$ eV. In addition, dimethylvinylamine, **R3**, has a lower electrophilicity power, $\omega=0.27$ eV, than ethylene, $\omega=0.73$ eV, the former being classified as a strong nucleophile.³⁴ Thus, the electrophilicity differences between **R1** and **R3**, $\Delta\omega=1.2$ eV, indicates a larger polar character for this cycloaddition that for the butadiene+ethylene one, $\Delta\omega=0.32$, that is classified as a pericyclic process.³⁴ Acylation of the nitrogen atom of the 1-aza-1,3-butadiene increases markedly the electrophilic character of **R2** relative **R1**, in agreement with the lowering of the activation energy. The electrophilicity power of **R2** is $\omega=2.14$ eV. Furthermore, the presence of the BH₃ coordinated to the *N*-acyl-1-aza-1,3-butadiene increases the electrophilicity power for **R2-B** to 3.24 eV, it being classified as a strong electrophile. In consequence, the LA catalyzed reaction between **R2-B** and **R3** presents a large $\Delta\omega=2.97$ eV, indicating a large ionic character for the bond-formation process.

Finally, the *N*-sulfonyl-1-aza-1,3-butadiene+methyl vinyl ether cycloaddition reaction presents an electrophilicity difference, $\Delta\omega=1.91$ eV, similar to that for the reaction between **R2** and **R3**. Although the vinyl ethers are less nucleophile than the vinylamines, the electrophilicity for dimethylvinylamine is lower than that for methyl vinyl ether (see Table 3), the larger electrophilicity for the *N*-sulfonyl-1-aza-1,3-butadiene than for the *N*-acyl-1-aza-derivative **R2** makes that both reactions present similar reactivity.

Since these cycloadditions have a large ionic character, an analysis of the electrophilic and nucleophilic Fukui functions³⁷ at the corresponding reactants allows explaining the regioselectivity experimentally observed.³⁵ In consequence, the local functions have been evaluated at the reactants, the 1ABDs **R1**, **R2** and **R2-B** and the vinylamine **R3**. The values of the Fukui functions are summarized in Table 4.

The asymmetric vinylamine **R3** has the largest nucleophilic

activation at the C5 position ($f_k^- = 0.41$) and, in consequence, this is the more reactive site for a nucleophilic attack. On the other hand, for the 1ABD systems there are three electrophilic positions, N1, C2 and C4 atoms. Although the C2 carbon atom that corresponds with the electrophilic carbon of an imine group has a large Fukui function value, it does not participate in these cycloadditions. Analysis of the Fukui function values for nucleophilic (+) attack at the ends of these 1ABD derivatives shows that the C4 carbon atoms have a larger Fukui function value than the N1 nitrogen atoms, indicating that the C4 carbon atoms are the more electrophilic centers. In consequence, the most favorable nucleophile/electrophile interaction between **R3** and the 1ABD derivatives **R1**, **R2** and **R2-B** will take place between the C5 carbon atom of dimethylvinylamine **R3** and the C4 carbon atom these 1ABDs in agreement with the *ortho* regioselectivity observed along the C4–C5 bond-formation.

Finally, the sum of the normalized Fukui functions of N1, C2, C3 and C4, 1.00 for **R1**, 0.84 for **R2** and 0.77 for **R2-B**, shows a decreasing of the accumulated Fukui functions for the nucleophilic attack at the 1ABD systems as a consequence of the presence of the conjugated electron-withdrawing acyl group on **R2** and **R2-B**. This result points out a favorable delocalization of the negative charge that is being transferred at the TSs that decreases activation energy, and they agree with the increase of the electrophilicity found for **R2** and **R2-B**.

5. Conclusions

The molecular mechanism for the cycloaddition reaction of 1-aza-1,3-butadiene and *N*-acyl-1-aza-1,3-butadiene with dimethylvinylamine has been studied using DFT methods at the B3LYP/6-31G* computational level. For these cycloadditions four reactive channels corresponding to the *endo* and *exo* approach modes of the nitrogen atom of the vinylamine to the 1-azabutadiene system along the *ortho* and *meta* regioisomeric possibilities are feasible. The results indicate these cycloadditions take place along a highly asynchronous concerted mechanism as a consequence of the large polarization of both reactants. Acylation of the nitrogen atom increases markedly the electrophilicity of the 1-azabutadiene system decreasing the activation energy. The reaction presents a large *ortho* regio and *endo* stereoselectivity in agreement with the experimental results. This formally [4+2] cycloaddition must be considered as the nucleophilic attack of the electron-rich vinylamine to the electron-poor *N*-acyl-1-azabutadiene system followed of a concomitant ring-closure. Inclusion of the BH₃ Lewis acid coordinated to the oxygen atom of the acyl substituent changes the mechanism from a concerted to a stepwise one because a large stabilization of the corresponding zwitterionic intermediate.

The natural population analysis at the corresponding TSs indicates that these cycloadditions have large polar character as a consequence of the large charge transfer from the electron-donor vinylamine to the electron-acceptor 1-aza-1,3-butadiene derivatives. However, the manifest decreasing of the activation energies for these cyclo-

additions can be understood as an increase the electrophilicity of these 1-azabutadiene derivatives as a consequence of the large charge delocalization at the acyl and BH₃-coordinated acyl substituents.

A DFT analysis performed on reactants shows that these cycloadditions take place along bond-formation processes with a large polar character. The charge transfer is therefore predicted to take place from the vinylamine acting as a nucleophile towards the end of the *N*-acyl-1-aza-1,3-butadiene derivatives as an electrophiles, as confirmed by the values of electronic chemical potential and charge transfer analysis at the corresponding TSs. In addition, the large Fukui function values at the ends of the reactants allow explaining the *ortho* regioselectivity observed. Finally, an analysis for the electrophilicity difference for the reactants of the *N*-sulfonyl-1-aza-1,3-butadiene+methyl vinyl ether cycloaddition reveals a similar pattern than for *N*-acyl-1-aza-1,3-butadiene+dimethylvinylamine one. Therefore, the main conclusions obtained from this DFT study can be widespread to the IEDDA reaction of *N*-sulfonyl-1-aza-1,3-butadienes acting as electrophiles with electron-rich vinyl ethers acting as nucleophiles.

Acknowledgements

This work was supported by research funds provided by the Ministerio de Educación y Cultura of the Spanish Government by DGICYT (project PB98-1429). All calculations were performed on a Cray-Silicon Graphics Origin 2000 of the Servicio de Informática de la Universidad de Valencia. I am most indebted to this center for providing us with computer capabilities.

References

1. Boger, D. L. *Tetrahedron* **1983**, *39*, 2869.
2. Weinred, S. M.; Scola, P. M. *Chem. Rev.* **1989**, *89*, 1525.
3. Tietze, L. F.; Ketschau, G. *Top. Curr. Chem.* **1997**, *189*, 1.
4. Hwang, Y. C.; Fowler, F. W. *J. Org. Chem.* **1985**, *50*, 2719.
5. Cheng, Y. S.; Lupo, A. T. J.; Fowler, F. W. *J. Am. Chem. Soc.* **1983**, *105*, 7696.
6. Boger, D. L.; Corbett, W. L.; Curran, T. T.; Kasper, A. M. *J. Am. Chem. Soc.* **1991**, *113*, 1713.
7. Boger, D. L.; Corbett, W. L.; Wiggins, J. M. *J. Org. Chem.* **1990**, *55*, 2999.
8. Boruah, R. C.; Ahmed, S.; Sharma, U.; Sandhu, J. S. *J. Org. Chem.* **2000**, *65*, 922.
9. Tran Huu Dau, M. E.; Flament, J.-P.; Lefour, J.-M.; Riche, C.; Grierson, D. S. *Tetrahedron Lett.* **1992**, *33*, 2343.
10. Bachrach, S. M.; Liu, M. *J. Org. Chem.* **1992**, *57*, 6736.
11. Park, Y. S.; Lee, B.-S.; Lee, I. *New J. Chem.* **1999**, *23*, 707.
12. Tietze, L. F.; Fennen, J.; Geibler, H.; Schulz, G.; Anders, E. *Liebigs Ann.* **1995**, 1681.
13. Gonzalez, J.; Houk, K. N. *J. Org. Chem.* **1992**, *57*, 3031.
14. Barluenga, J.; Sordo, T. L.; Sordo, J. A.; Fustero, S.; González, J. *J. Mol. Struct. (Theochem.)* **1994**, *315*, 63.
15. Venturini, A.; Joglar, J.; Fustero, S.; Gonzalez, J. *J. Org. Chem.* **1997**, *62*, 3919.
16. Melo, T. M. V. D. P. E.; Fausto, R.; Gonsalves, A. M. D. R.; Gilchrist, T. L. *J. Org. Chem.* **1998**, *63*, 5350.

17. Augusti, R.; Gozzo, F. C.; Moraes, L. A. B.; Sparrapan, R.; Eberlin, M. N. *J. Org. Chem.* **1998**, *63*, 4889.
18. Avalos, M.; Babiano, R.; Cintas, P.; Clemente, F. R.; Jiménez, J. L.; Palacios, J. C.; Sánchez, J. B. *J. Org. Chem.* **1999**, *64*, 6297.
19. Avalos, M.; Babiano, R.; Clemente, F. R.; Cintas, P.; Gordillo, R.; Jiménez, J. L.; Palacios, J. C. *J. Org. Chem.* **2000**, *65*, 8251.
20. Jursic, B. S.; Zdravkovski, Z. *J. Comput. Chem.* **1996**, *17*, 298.
21. Domingo, L. R. *J. Org. Chem.* **2001**, *66*, 3211.
22. Domingo, L. R.; Oliva, M.; Andrés, J. *J. Org. Chem.* **2001**, *66*, 6151.
23. Domingo, L. R.; Jones, R. A.; Picher, M. T.; Sepúlveda-Arqués, J. *Tetrahedron* **1995**, *51*, 8739.
24. Domingo, L. R.; Picher, M. T.; Andrés, J.; Moliner, V.; Safont, V. S. *Tetrahedron* **1996**, *52*, 10693.
25. Domingo, L. R.; Picher, M. T.; Andrés, J.; Safont, V. S. *J. Org. Chem.* **1997**, *62*, 1775.
26. Domingo, L. R.; Picher, M. T.; Zaragoza, R. J. *J. Org. Chem.* **1998**, *63*, 9183.
27. Domingo, L. R.; Arnó, M.; Andrés, J. *J. Org. Chem.* **1999**, *64*, 5867.
28. Domingo, L. R.; Picher, M. T.; Aurell, M. J. *J. Phys. Chem. A* **1999**, *103*, 11425.
29. Parr, R. G.; Pearson, R. G. *J. Am. Chem. Soc.* **1983**, *105*, 7512.
30. Parr, R. G.; Yang, W. *Density Functional Theory of Atoms and Molecules*; Oxford University: New York, 1989.
31. Ziegler, T. *Chem. Rev.* **1991**, *91*, 651.
32. Pearson, R. G. *Chemical Hardness, Applications from Molecules to Solids*; Wiley-VHC/Verlag GMBH: Weinheim, 1997.
33. Parr, R. G.; von Szentpaly, L.; Liu, S. *J. Am. Chem. Soc.* **1999**, *121*, 1922.
34. Domingo, L. R.; Aurell, M. J.; Pérez, P.; Contreras, R. *Tetrahedron*, **2002**, in press.
35. Domingo, L. R.; Aurell, M. J. *J. Org. Chem.* **2002**, *67*, 959.
36. Domingo, L. R.; Arnó, M.; Contreras, R.; Pérez, P. *J. Phys. Chem. A* **2002**, *106*, 952.
37. Parr, R. G.; Yang, W. *J. Am. Chem. Soc.* **1984**, *106*, 4049.
38. Becke, A. D. *J. Chem. Phys.* **1993**, *98*, 5648.
39. Lee, C.; Yang, W.; Parr, R. G. *Phys. Rev. B* **1988**, *37*, 785.
40. Hehre, W. J.; Radom, L.; Schleyer, P. v. R.; Pople, J. A. *Ab initio Molecular Orbital Theory*; Wiley: New York, 1986.
41. Schlegel, H. B. *J. Comput. Chem.* **1982**, *3*, 214.
42. Schlegel, H. B. Geometry Optimization on Potential Energy Surface. In *Modern Electronic Structure Theory*, Yarkony, D. R., Ed.; World Scientific: Singapore, 1994.
43. Fukui, K. *J. Phys. Chem.* **1970**, *74*, 4161.
44. González, C.; Schlegel, H. B. *J. Phys. Chem.* **1990**, *94*, 5523.
45. González, C.; Schlegel, H. B. *J. Chem. Phys.* **1991**, *95*, 5853.
46. Reed, A. E.; Weinstock, R. B.; Weinhold, F. *J. Chem. Phys.* **1985**, *83*, 735.
47. Reed, A. E.; Curtiss, L. A.; Weinhold, F. *Chem. Rev.* **1988**, *88*, 899.
48. Frisch, M. J.; Trucks, G. W.; Schlegel, H. B.; Scuseria, G. E.; Robb, M. A.; Cheeseman, J. R.; Zakrzewski, V. G.; Montgomery, Jr. J. A.; Stratmann, R. E.; Burant, J. C.; Dapprich, S.; Millam, J. M.; Daniels, A. D.; Kudin, K. N.; Strain, M. C.; Farkas, O.; Tomasi, J.; Barone, V.; Cossi, M.; Cammi, R.; Mennucci, B.; Pomelli, C.; Adamo, C.; Clifford, S.; Ochterski, J.; Petersson, G. A.; Ayala, P. Y.; Cui, Q.; Morokuma, K.; Malick, D. K.; Rabuck, A. D.; Raghavachari, K.; Foresman, J. B.; Cioslowski, J.; Ortiz, J. V.; Stefanov, B. B.; Liu, G.; Liashenko, A.; Piskorz, P.; Komaromi, I.; Gomperts, R.; Martin, R. L.; Fox, D. J.; Keith, T.; Al-Laham, M. A.; Peng, C. Y.; Nanayakkara, A.; Gonzalez, C.; Challacombe, M.; Gill, P. M. W.; Johnson, B.; Chen, W.; Wong, M. W.; Andres, J. L.; Gonzalez, C.; Head-Gordon, M.; Replogle, E. S.; Pople, J. A. *Gaussian98*, Revision A.6; Gaussian, Inc.: Pittsburgh PA, 1998.
49. Tomasi, J.; Persico, M. *Chem. Rev.* **1994**, *94*, 2027.
50. Simkin, B. Y.; Shekhet, I. *Quantum Chemical and Statistical Theory of Solutions—A Computational Approach*; Ellis Horwood: London, 1995.
51. Cancès, M. T.; Mennucci, V.; Tomasi, J. *J. Chem. Phys.* **1997**, *107*, 3032.
52. Cossi, M.; Barone, V.; Cammi, R.; Tomasi, J. *Chem. Phys. Lett.* **1996**, *255*, 327.
53. Barone, V.; Cossi, M.; Tomasi, J. *J. Comput. Chem.* **1998**, *19*, 404.
54. Contreras, R.; Fuentealba, P.; Galván, M.; Pérez, P. *Chem. Phys. Lett.* **1999**, *304*, 405.
55. Fuentealba, P.; Pérez, P.; Contreras, R. *J. Chem. Phys.* **2000**, *113*, 2544.
56. Wiberg, K. B. *Tetrahedron* **1968**, *24*, 1083.
57. Kahn, S. D.; Hehre, W. J.; Pople, J. A. *J. Am. Chem. Soc.* **1987**, *109*, 1871.
58. Domingo, L. R. *Theor. Chem. Acc.* **2000**, *104*, 240.
59. Yamabe, S.; Minato, T. *J. Org. Chem.* **2000**, *65*, 1830.